THE JOURNAL OF PHYSICAL CHEMISTRY A

pubs.acs.org/JPCA Article

Tag-Free, Temperature Dependent Infrared Spectra of the GFP Chromophore: Revisiting the Question of Isomerism

Wyatt Zagorec-Marks, Madison M. Foreman, and J. Mathias Weber*

Cite This: J. Phys. Chem. A 2020, 124, 7827−7831 Read Online

ACCESS | Metrics & More | Article Recommendations

ABSTRACT: We report infrared spectra of a model chromophore of green fluorescent protein, prepared in an ion trap at temperatures ranging from 30 K to room temperature. We compare the changes in the infrared spectrum with predicted infrared spectra for the *Z* and *E* isomers of this molecule, and we confirm that the molecule exists as the *Z* isomer at low temperatures. We revisit the question whether or not it can thermally isomerize in the temperature range of this experiment, and we find no evidence for isomerization.

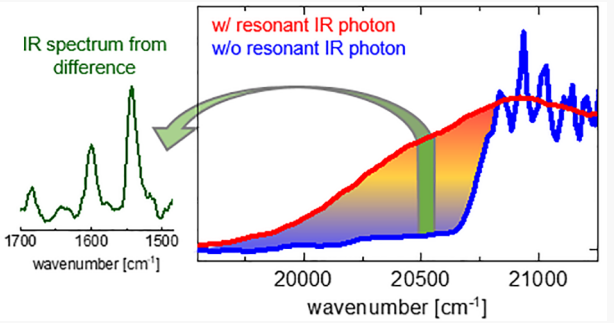

INTRODUCTION

Many of the properties of complex molecules are well-known in condensed phases, but their intrinsic structural and electronic characteristics, i.e., in the absence of solvent or other chemical environments, present a challenge. For ionic species, photodissociation spectroscopy of mass-selected ions provides one of the cleanest possible ways to access their intrinsic photophysics, as well as the elucidation of key structural elements such as intramolecular hydrogen bonds[1−4] and isomerization.[4−6] Last, but not least, spectroscopic studies in this vein yield benchmark data for testing computational predictions.

In the visible and UV regions of the electromagnetic spectrum, absorption of one or two photons is often sufficient to lead to photodissociation of a given molecule, but photodissociation is less accessible for infrared (IR) spectroscopy since the bond dissociation energy of most molecules is much greater than the energy deposited by the absorption of one or two photons. Combining IR and UV/vis excitation steps (IR-UV double resonance) leads to a powerful set of methods to investigate the structures and infrared spectra of molecules, free from the limitations on ion temperature and common difficulties in the preparation of tagged species in messenger tagging approaches or the technical requirements and nonlinearities encountered in infrared multiphoton dissociation spectroscopy (IRMPD). In IR-UV double resonance spectroscopy, the target molecule absorbs an infrared photon first and is then irradiated by a second light source operating in the UV or visible spectral region, leading to photodissociation after one or multiple absorption events on electronic transitions. There are several variations of this approach (see, e.g., refs 7−10), summarized in Figure 1. One is

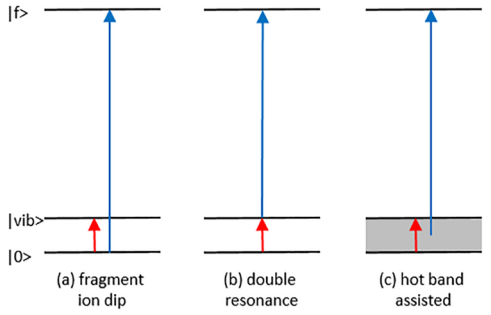

Figure 1. Excitation schemes for resonant IR-UV 2-photon photodissociation spectroscopy. Fragmentation occurs upon excitation to state $|f\rangle$.

to tune the UV/vis light source to a specific, narrow transition $|0\rangle \rightarrow |f\rangle$ starting from the ground state, $|0\rangle$, where fragmentation occurs upon excitation into the fragmenting final state $|f\rangle$. Monitoring the fragment ion signal upon bleaching the ground state population by the infrared absorption step then shows infrared absorptions as dips in the fragment ion signal (IR-UV ion dip spectroscopy, Figure 1a). Another technique is to tune the UV/vis light source to be resonant with the transition $(|vib\rangle \rightarrow |f\rangle)$ from a specific

Received: August 5, 2020
Revised: August 28, 2020
Published: August 31, 2020

https://dx.doi.org/10.1021/acs.jpca.0c07172
J. Phys. Chem. A 2020, 124, 7827−7831

vibrationally excited state $|vib\rangle$ to a specific vibronic resonance in the fragmenting state $|f\rangle$ (true IR-UV double resonance, Figure 1b).

In the present work, we use a double resonance approach that works particularly well for relatively large ions.[10] In this approach, the target molecule undergoes rapid intramolecular vibrational relaxation (IVR) after absorption of an infrared photon. This process essentially produces a hot ion, although the distribution of energy is not necessarily thermal and depends on the time after absorption. Tuning the UV/vis photon energy to a region where hot bands are found in the UV/vis photodissociation spectrum results in excitation to the fragmenting state $|f\rangle$ (Figure 1c). We will refer to this method as hot band assisted IR (HAIR) spectroscopy; it is sometimes also called IR-UV gain spectroscopy in the literature. This method has been less widely used than other IR-UV double resonance methods, but it has been employed for the spectroscopy of large molecules, which have a sufficiently large vibrational density of states to facilitate efficient IVR.

We use it here to perform infrared spectroscopy at different temperatures on deprotonated *p*-hydroxybenzylidene-2,3-dimethylimidazoline (HBDI$^-$, see Scheme 1), a model chromophore for the green fluorescent protein (GFP). We compare the HAIR spectra with spectra obtained in previous work[11] by messenger tagging, and we revisit the question of isomerism in HBDI$^-$ at elevated temperatures. The main motivation for using this method to investigate HBDI$^-$ is that it has two isomers (*Z* and *E*, see Scheme 1). The *Z* isomer is lower in energy by ca. 100 meV and is the only isomer that is significantly populated at cryogenic temperatures. The barrier to interconversion has been calculated to be 1.24 eV, which would be too high for thermal isomerization at room temperature.[12] However, the *E* isomer has been discovered in room temperature ion mobility experiments.[12] Earlier IRMPD spectroscopy experiments carried out at room temperature[13] were inconclusive regarding the identification of the isomer. In our own recent work,[11] we found that the S_1 region of the spectrum of HBDI$^-$ depends strongly on the temperature, and we raised the hypothesis that this could be due to the population of the *E* isomer at temperatures above 180 K. We revisit the question of isomerism in HBDI$^-$ in the present article.

Scheme 1. *Z* and *E* Isomers of HBDI$^-$

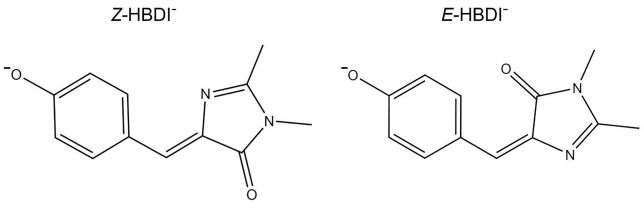

METHODS

The experimental apparatus has been described in detail in previous work.[14] Briefly summarized, we electrosprayed methanolic solutions of HBDI, with the pH adjusted to 11–12 by addition of aqueous KOH solution, using N_2 as nebulizing gas. The electrosprayed microdroplets are desolvated in a heated capillary, and after passing a skimmer, the resulting ions are guided through several differential pumping stages using octopole ion guides. The ions are then captured in a temperature-controlled 3D quadrupole trap, where they are allowed to collide with D_2 buffer gas for 50 ms to bring them to temperatures close to the trap temperature. Subsequently, the contents of the trap are injected into a time-of-flight mass spectrometer where we mass select the HBDI$^-$ ions using a pulsed mass gate. The mass selected ions can then be irradiated with the output of two tunable optical parametric converter systems, each with pulse durations of 5–7 ns. A BBO based optical parametric oscillator (OPO) with a bandwidth of ca. 5 cm^{-1} provides the light for spectroscopy in the visible range, while a KTP/KTA/$AgGaSe_2$ based optical parametric converter system with a bandwidth of ca. 2 cm^{-1} generates infrared radiation for vibrational excitation. The infrared and visible light beam paths are spatially separated by 8 cm, and the infrared pulse is irradiating the target molecules ca. 1.5 μs before the visible pulse (parent ion kinetic energies are ca. 3.2 keV, the mass of the ion is 215 u). Dissociation by loss of a CH_3 fragment upon absorption of two photons in the visible is detected using a reflectron for secondary mass analysis and monitoring the fragment mass with 200 u, employing a microchannel plate detector for ion detection. The mass spectrometer and the visible OPO are operated at a repetition rate of 20 Hz, and the infrared light source is fired every other experimental cycle (10 Hz) to allow subtraction of background from unimolecular decay and electronic excitation by monitoring of fragment ion signal with and without infrared irradiation. All spectra were corrected for photon fluence.

We use geometries and harmonic frequency calculations (scaled by 0.98) for the ground state of each isomer calculated using density functional theory (DFT) with the B3LYP functional[15] and a def2-TZVPP basis set for all atoms[16] All calculations were carried out employing the Gaussian 16 program suite[17] and were published in earlier work from our group.[11]

RESULTS AND DISCUSSION

The onset of the photodissociation spectrum of HBDI$^-$ is presented in Figure 2 at 30 K and at 300 K, focusing on the region of the $S_0 \rightarrow S_1$ band origin at 20 930 cm^{-1}.[11] The

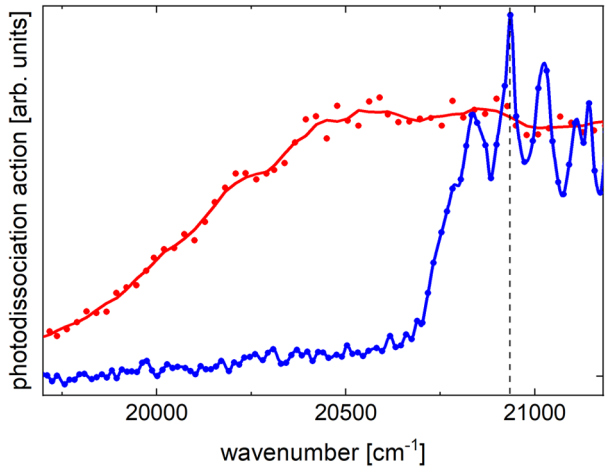

Figure 2. UV–vis spectra of HBDI$^-$ at 300 K (red trace) and 30 K (blue trace) in the band origin region. The dots are data points, the full lines are a 5-point adjacent average (300 K) and an Akima spline (30 K) to guide the eye. The dashed vertical line shows the band origin of the $S_0 \rightarrow S_1$ band at 20 930 cm^{-1}.

https://dx.doi.org/10.1021/acs.jpca.0c07172
J. Phys. Chem. A 2020, 124, 7827–7831

spectra were acquired by irradiation of $HBDI^-$ ions with laser pulses in the visible spectral region, without prior exposure to infrared pulses. Comparison of the two spectra reveals that the spectral region below ca. 20 700 cm^{-1} contains only hot bands, and shows no absorption features at low temperatures. The spectrum acquired at 30 K shows pronounced vibrational structure in the S_1 state,[11] which is not resolved in the spectrum at 300 K.

In the HAIR approach, we use the region containing only hot bands as a probe for infrared spectroscopy. Absorption of an infrared photon prior to electronic excitation adds vibrational energy into the molecule, and leads to an increased intensity of hot bands, compared to irradiation in the visible only, as documented in Figure 3. The infrared-generated hot bands are observable for all trap temperatures studied here, from 30 to 300 K. This allows us to record the infrared spectra of $HBDI^-$ at different temperatures (Figure 4). This would not be feasible relying on messenger tagging, given the narrow range of trap temperatures where messenger species can be attached to the ion (e.g., typically 25−40 K for N_2 tagging in our setup). We note that the infrared-generated hot band signals are more pronounced at low trap temperature than at high temperature, and the signal-to-noise ratio is correspondingly higher at low temperature.

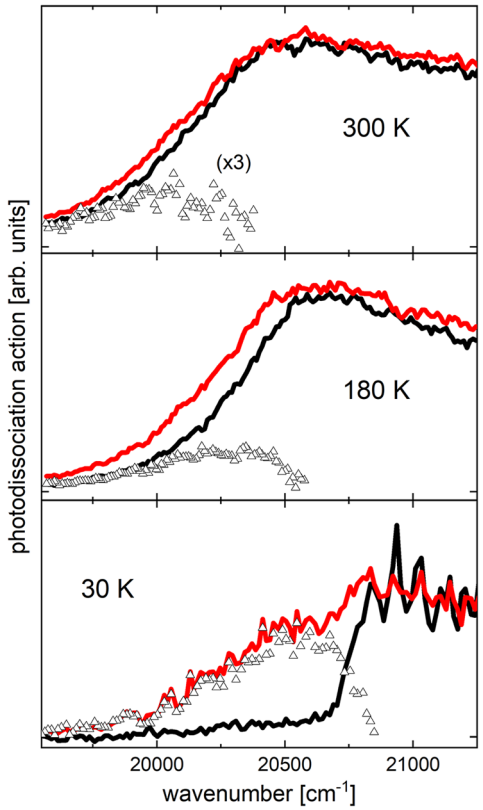

Figure 3. Photodissociation spectra in the S_1 band origin region of $HBDI^-$ at 30, 180, and 300 K trap temperatures. Full lines are spectra without (black) and with (red) resonant IR irradiation at 1536 cm^{-1}; open triangles show the difference between the two signals, where the difference values for 300 K have been amplified by a factor 3 for clarity.

In the following, we use our assignment of vibrational modes as published earlier.[11] The comparison of the IR spectrum obtained by N_2 tagging[11] with HAIR data at 30 K trap

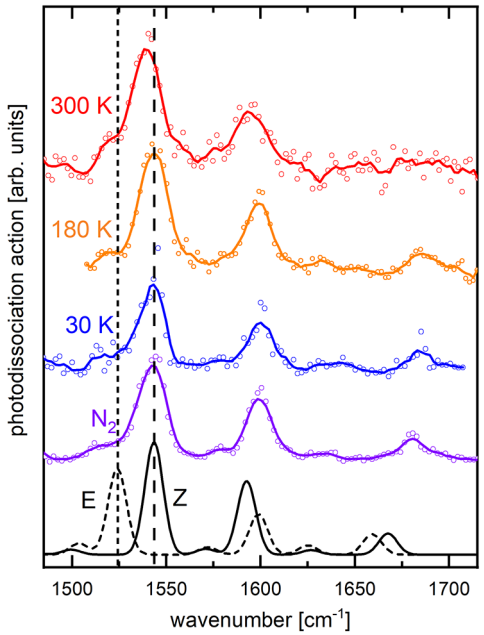

Figure 4. Infrared spectra of $HBDI^-$ under different conditions. The lowest traces are simulated spectra for the dominant Z isomer (full black line) and the E isomer (dotted black line). The other traces show experimental infrared spectra using N_2 tagging and HAIR data for different trap temperatures as indicated on the traces. Open circles are raw data points, the full lines are 5-point adjacent averages. The vertical lines show the calculated band positions of the dominant band for the Z and E isomers. The data for N_2 tagged $HBDI^-$ were taken from ref.[11] The HAIR spectra were acquired at 20 580, 20 160, and 19 800 cm^{-1} for 30, 180, and 300 K trap temperature, respectively.

temperature (see Figure 4) shows that the N_2 tag does not influence the peaks at 1544 and 1600 cm^{-1} within our experimental resolution, both belonging to in-plane CH bending/imidazole ring deformation modes. The imidazole CO stretching signature around 1680 cm^{-1} shows a weak tag-induced shift of −5 cm^{-1}. The weak phenolate CO stretching/ring deformation mode at 1578 cm^{-1} is not significantly affected by N_2 tagging. The phenolate CO stretching/bridge deformation mode at 1632 cm^{-1} shifts by −8 cm^{-1} upon N_2 tagging.

The HAIR spectra show a weak temperature dependence of the infrared signatures (see Figure 4). The dominant band at 1544 cm^{-1} shifts by −5 cm^{-1} between 30 and 300 K trap temperature. Similarly, the band at 1600 cm^{-1} shifts by −7 cm^{-1} in the same temperature range. Interestingly, both shifts are nearly indiscernible at 180 K, which is an important observation in the context of thermal isomerization (vide infra). The peak at 1680 cm^{-1} broadens significantly with increasing temperature, and is not clearly observable at 300 K.

The decreasing sensitivity of HAIR spectroscopy with increasing temperature can be qualitatively understood in terms of the temperature dependence of the vibrational molecular heat capacity, assuming in a very simple model that IVR results in a thermal distribution of energy throughout the vibrational modes of the molecule at the time of irradiation with the visible light pulse. Figure 5 shows the vibrational contributions to internal energy (U_{vib}) and constant volume heat capacity ($C_{V,vib}$) of $HBDI^-$ over the range of 20−300 K. The vibrational internal energy was calculated from

https://dx.doi.org/10.1021/acs.jpca.0c07172
J. Phys. Chem. A 2020, 124, 7827−7831

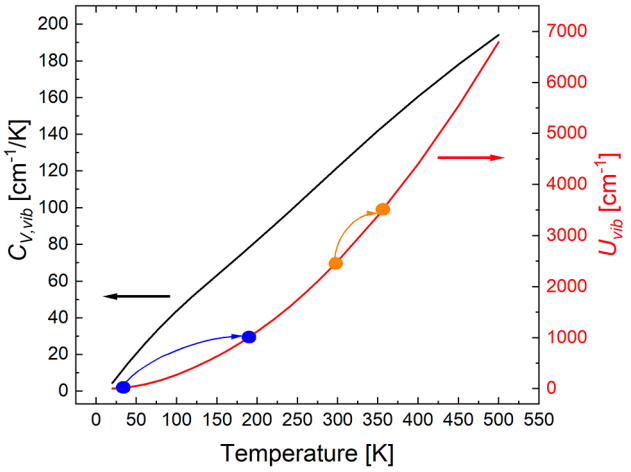

Figure 5. Constant volume heat capacity (black trace) and average vibrational internal energy (red trace) of HBDI$^-$ as a function of temperature. The circles and curved arrows show the change in molecular temperature upon absorption of a 1000 cm^{-1} infrared photon, starting from 30 K (blue) and from 300 K (orange). The horizontal arrows indicate which curve belongs to which vertical scale.

$$U_{\text{vib}} = \sum_j \frac{\hbar\omega_j}{e^{\hbar\omega_j/k_B T} - 1} \quad (1)$$

where the ω_j are frequencies of the vibrational modes (obtained from harmonic frequency calculations), $\hbar$ is the reduced Planck constant, k_B is the Boltzmann constant, and T is the temperature. The constant volume heat capacity ($C_{V,vib}$) is simply the temperature derivative of the internal energy. Considering absorption of an infrared photon with frequency 1000 cm^{-1}, Figure 5 shows that upon IVR this increase in vibrational energy will cause a substantial change in the molecular temperature, if we assume an initial temperature of 30 K. This change is less pronounced for a higher initial temperature as $C_{V,vib}$ increases, showing why the photon-induced increase in hot band intensity will be in general more difficult to measure at higher initial temperatures. This issue will be exacerbated when dealing with larger molecules, which have larger heat capacities to begin with.

In our previous work on electronic spectroscopy of HBDI$^-$,[11] we observed a significant difference between the S_1 photodissociation spectra at low and high trap temperatures. The spectrum at 30 K can be described well by Franck–Condon simulations, while at temperatures of 180 K and higher, any such description fails to recover the observed high intensities in the hot-band region, or the fact that the apparent peak of the S_1 photodissociation spectrum shifts to the red at high temperatures (see also Figures 2 and 3). We had raised the hypothesis[11] that this could be due to an increase in the relative population of the E isomer with temperature, as the E isomer of HBDI$^-$ has been previously observed in ion mobility experiments.[12] While the infrared spectrum of HBDI$^-$ (Figure 4) changes slightly with temperature, this change is insufficient to infer a drastic change in isomer populations needed to describe the temperature dependence of the electronic spectrum. In particular, our assignment of the Z isomer being responsible for the cryogenic spectrum of HBDI$^-$ (tagged or tag-free) is based primarily on the spacing of the three dominant signatures at 1544, 1600, and 1680 cm^{-1}. If the E isomer were to become significantly populated at 180 K, we would expect the signatures to change. In particular, the E isomer should develop a strong signature at ca. 1520 cm^{-1}, while the peak at 1600 cm^{-1} should exhibit a high-energy shoulder. While there is a weak feature at 1512 cm^{-1}, this band has been identified as the signature of a phenolate in-plane CH bending/phenolate deformation mode.[11] It is present for all temperatures, its relative intensity at 180 K is not enhanced compared to 30 K, and the spacing between the three main components of the spectrum does not change appreciably at 180 K. The temperature dependent HAIR spectra therefore cannot substantiate the hypothesis that the E isomer is thermally populated, consistent with a barrier to interconversion of 1.24 eV,[12] which would preclude isomerization at room temperature. The weak apparent red shift of the bands at 1544 and 1600 cm^{-1} is most likely caused by vibrational hot bands, i.e., by vibrational transitions beginning in thermally excited states of low-energy modes of the molecule.

Regarding the temperature dependence of the electronic spectrum of HBDI$^-$, our observations[11] of spectroscopic signatures that were not recovered by simple hot band behavior are reminiscent of those by Roithova and co-workers[18] who found a pronounced temperature dependence of the photodissociation spectra of rhodamine 123 on the ion temperature, which was also not recoverable by Franck–Condon simulations. For that molecule, the authors concluded that the cause of the temperature dependence for rhodamine 123 lies in the fact that photodissociation required 3–4 photons. Efficient return to the ground state after successive absorption events (by nonradiative processes or by fluorescence) resulted in an increase of vibrational temperature for the absorption of all photons after the first, which skewed the spectrum toward lower photon energies. These effects cannot be accounted for by Franck–Condon simulations. We assume that similar processes are at play in HBDI$^-$, since the molecule requires the absorption of two photons for photodissociation in the S_1 region.[11] Fluorescence is not an active relaxation pathway for bare HBDI$^-$, but HBDI$^-$ undergoes radiationless relaxation with ps lifetime[19−25] after absorption of the first photon, resulting in the population of a highly vibrationally excited electronic ground state, which will then absorb the second photon. As the vibrational energy content of the molecule before the absorption of the second photon will be many thousands of cm^{-1}, the simple approach of Franck–Condon simulations is likely to fail in predicting the spectral envelope.

CONCLUSIONS

We use hot band assisted infrared spectroscopy to probe the temperature dependence of the isomerism of HBDI$^-$ prepared in a temperature-controlled ion trap between 30 and 300 K. Messenger tagging results in very small changes of the vibrational spectrum compared to the tag free spectrum at the same trap temperature. We find no evidence of a significant change in isomer population with increasing temperature and conclude that there is no thermal conversion from the Z to the E isomer in our experiment, consistent with the literature values calculated for the barrier to interconversion. Therefore, we attribute the observation of the E isomer in ion mobility experiments[12] to experimental conditions where the E isomer is generated early in the ion preparation process, and subsequently kinetically trapped. Experiments combining ion mobility and IR spectroscopy[26,27] could provide more clarity.

https://dx.doi.org/10.1021/acs.jpca.0c07172
J. Phys. Chem. A 2020, 124, 7827−7831

AUTHOR INFORMATION

Corresponding Author

J. Mathias Weber − *JILA and Department of Chemistry, University of Colorado, Boulder, Colorado 80309-0440, United States;* orcid.org/0000-0002-5493-5886; Phone: +1-303-492-7841; Email: weberjm@jila.colorado.edu

Authors

Wyatt Zagorec-Marks − *JILA and Department of Chemistry, University of Colorado, Boulder, Colorado 80309-0440, United States*

Madison M. Foreman − *JILA and Department of Chemistry, University of Colorado, Boulder, Colorado 80309-0440, United States*

Complete contact information is available at: https://pubs.acs.org/10.1021/acs.jpca.0c07172

Notes

The authors declare no competing financial interest.

ACKNOWLEDGMENTS

We gratefully acknowledge support from the U.S. National Science Foundation under Award No. CHE-1764191 and the NSF Physics Frontier Center at JILA (Award No. PHY-1734006). We also thank Drs. Stephen R. Meech and Philip C. B. Page (University of East Anglia, U.K., grant support through EPSCR Grants EP/E010466 and EP/H025715) for providing us with the *p*-hydroxybenzylidene-2,3-dimethylimidazolinone samples that were used in this work, and we thank Dr. Jan R. R. Verlet (University of Durham, U.K.) for much helpful discussion.

REFERENCES

(1) Kamrath, M. Z.; Relph, R. A.; Guasco, T. L.; Leavitt, C. M.; Johnson, M. A. Vibrational predissociation spectroscopy of the H_2-tagged mono- and dicarboxylate anions of dodecanedioic acid. *Int. J. Mass Spectrom.* **2011**, *300*, 91−98.

(2) Marsh, B. M.; Duffy, E. M.; Soukup, M. T.; Zhou, J.; Garand, E. Intramolecular Hydrogen Bonding Motifs in Deprotonated Glycine Peptides by Cryogenic Ion Infrared Spectroscopy. *J. Phys. Chem. A* **2014**, *118*, 3906−3912.

(3) DeBlase, A. F.; Kass, S. R.; Johnson, M. A. On the character of the cyclic ionic H-bond in cryogenically cooled deprotonated cysteine. *Phys. Chem. Chem. Phys.* **2014**, *16*, 4569−4575.

(4) Leavitt, C. M.; Wolk, A. B.; Fournier, J. A.; Kamrath, M. Z.; Garand, E.; Van Stipdonk, M. J.; Johnson, M. A. Isomer-Specific IR−IR Double Resonance Spectroscopy of D_2-Tagged Protonated Dipeptides Prepared in a Cryogenic Ion Trap. *J. Phys. Chem. Lett.* **2012**, *3*, 1099−1105.

(5) Dean, J. C.; Walsh, P. S.; Biswas, B.; Ramachandran, P. V.; Zwier, T. S. Single-conformation UV and IR spectroscopy of model G-type lignin dilignols: the *β*−O−4 and *β*−*β* linkages. *Chem. Sci.* **2014**, *5*, 1940−1955.

(6) Kirschbaum, C.; Saied, E. M.; Greis, K.; Mucha, E.; Gewinner, S.; Schollkopf, W.; Meijer, G.; Helden, G.; Poad, B. L. J.; Blanksby, S. J.; Arenz, C.; Pagel, K.; et al. Resolving Sphingolipid Isomers Using Cryogenic Infrared Spectroscopy. *Angew. Chem., Int. Ed.* **2020**, *59*, 13638−13642.

(7) Inokuchi, Y.; Ebata, T.; Rizzo, T. R. UV and IR Spectroscopy of Transition Metal−Crown Ether Complexes in the Gas Phase: Mn^{2+}(benzo-15-crown-5)$(H_2O)_{0-2}$. *J. Phys. Chem. A* **2019**, *123*, 6781−6786.

(8) Shubert, V. A.; Zwier, T. S. IR−IR−UV Hole-Burning: Conformation Specific IR Spectra in the Face of UV Spectral Overlap. *J. Phys. Chem. A* **2007**, *111*, 13283−13286.

(9) Burke, N. L.; Redwine, J. G.; Dean, J. C.; McLuckey, S. A.; Zwier, T. S. UV and IR spectroscopy of cold protonated leucine enkephalin. *Int. J. Mass Spectrom.* **2015**, *378*, 196−205.

(10) Nagornova, N. S.; Rizzo, T. R.; Boyarkin, O. V. Exploring the Mechanism of IR−UV Double-Resonance for Quantitative Spectroscopy of Protonated Polypeptides and Proteins. *Angew. Chem., Int. Ed.* **2013**, *52*, 6002−6005.

(11) Zagorec-Marks, W.; Foreman, M. M.; Verlet, J. R. R.; Weber, J. M. Cryogenic Ion Spectroscopy of the Green Fluorescent Protein Chromophore in Vacuo. *J. Phys. Chem. Lett.* **2019**, *10*, 7817−7822.

(12) Carrascosa, E.; Bull, J. N.; Scholz, M. S.; Coughlan, N. J. A.; Olsen, S.; Wille, U.; Bieske, E. J. Reversible Photoisomerization of the Isolated Green Fluorescent Protein Chromophore. *J. Phys. Chem. Lett.* **2018**, *9*, 2647−2651.

(13) Almasian, M.; Grzetic, J.; Berden, G.; Bakker, B.; Buma, W. J.; Oomens, J. Gas-phase infrared spectrum of the anionic GFP-chromophore. *Int. J. Mass Spectrom.* **2012**, *330*−*332*, 118−123.

(14) Xu, S.; Gozem, S.; Krylov, A. I.; Christopher, C. R.; Mathias Weber, J. Ligand influence on the electronic spectra of monocationic copper-bipyridine complexes. *Phys. Chem. Chem. Phys.* **2015**, *17*, 31938−31946.

(15) Lee, C.; Yang, W.; Parr, R. G. Development of the Colle-Salvetti correlation-energy formula into a functional of the electron density. *Phys. Rev. B: Condens. Matter Mater. Phys.* **1988**, *37*, 785−789.

(16) Weigend, F.; Ahlrichs, R. Balanced basis sets of split valence, triple zeta valence and quadruple zeta valence quality for H to Rn: Design and assessment of accuracy. *Phys. Chem. Chem. Phys.* **2005**, *7*, 3297−3305.

(17) Frisch, M. J.; et al. *Gaussian 16*, revision C.01; Gaussian Inc.: Wallingford, CT, 2016.

(18) Navrátil, R.; Jašík, J.; Roithová, J. Visible photodissociation spectra of gaseous rhodamine ions: Effects of temperature and tagging. *J. Mol. Spectrosc.* **2017**, *332*, 52−58.

(19) Mandal, D.; Tahara, T.; Meech, S. R. Excited-State Dynamics in the Green Fluorescent Protein Chromophore. *J. Phys. Chem. B* **2004**, *108*, 1102−1108.

(20) Litvinenko, K. L.; Webber, N. M.; Meech, S. R. Internal Conversion in the Chromophore of the Green Fluorescent Protein: Temperature Dependence and Isoviscosity Analysis. *J. Phys. Chem. A* **2003**, *107*, 2616−2623.

(21) Voliani, V.; Bizzarri, R.; Nifosì, R.; Abbruzzetti, S.; Grandi, E.; Viappiani, C.; Beltram, F. Cis−Trans Photoisomerization of Fluorescent-Protein Chromophores. *J. Phys. Chem. B* **2008**, *112*, 10714−10722.

(22) Horke, D. A.; Verlet, J. R. R. Photoelectron spectroscopy of the model GFP chromophore anion. *Phys. Chem. Chem. Phys.* **2012**, *14*, 8511−8515.

(23) Mooney, C. R. S.; Horke, D. A.; Chatterley, A. S.; Simperler, A.; Fielding, H. H.; Verlet, J. R. R. Taking the green fluorescence out of the protein: dynamics of the isolated GFP chromophore anion. *Chem. Sci.* **2013**, *4*, 921−927.

(24) Bochenkova, A. V.; Andersen, L. H. Ultrafast dual photoresponse of isolated biological chromophores: link to the photoinduced mode-specific non-adiabatic dynamics in proteins. *Faraday Discuss.* **2013**, *163*, 297−319.

(25) Anstöter, C. S.; Bull, J. N.; Verlet, J. R. R. Ultrafast dynamics of temporary anions probed through the prism of photodetachment. *Int. Rev. Phys. Chem.* **2016**, *35*, 509−538.

(26) Marianski, M.; Seo, J.; Mucha, E.; Thomas, D. A.; Jung, S.; Schlögl, R.; Meijer, G.; Trunschke, A.; von Helden, G. Structural Characterization of Molybdenum Oxide Nanoclusters Using Ion Mobility Spectrometry−Mass Spectrometry and Infrared Action Spectroscopy. *J. Phys. Chem. C* **2019**, *123*, 7845−7853.

(27) Warnke, S.; Ben Faleh, A.; Scutelnic, V.; Rizzo, T. R. Separation and Identification of Glycan Anomers Using Ultrahigh-Resolution Ion-Mobility Spectrometry and Cryogenic Ion Spectroscopy. *J. Am. Soc. Mass Spectrom.* **2019**, *30*, 2204−2211.